

# Supporting Information

Weigel et al. 10.1073/pnas.1315202110

## SI Text

### Clathrin-Coated Pit Lifetime Analysis

Clathrin-coated pits (CCPs) were analyzed in terms of their lifetimes following the work of Loerke et al. (1). The lifetime of a CCP is determined from the appearance and disappearance of a clathrin fluorescence spot in the total internal reflection fluorescence (TIRF) field of view. Some trajectories may both appear and disappear within the movie recording total time, but others may be truncated by the movie start or finish. For instance, if a CCP initiates before the start of the movie, an unknown portion of the beginning of the cycle is missing. In the case of a trajectory that is recorded in its full length, its lifetime equals the length of the trajectory. However, when the trajectory is truncated, the lifetime is unknown. Thus, the estimation of relative frequency of lifetimes is biased toward smaller times. This bias depends in turn on the movie length. Assuming a particle appears with equal probability at any point in time, for a given movie of duration  $\tilde{T}$ , the probability of a pit with lifetime  $\tilde{l}$  to be truncated by the end of the movie recording is  $c(\tilde{l}, \tilde{T}) = (1 + \tilde{l})/\tilde{T}$  for  $\tilde{l} < \tilde{T}$ . The units of  $\tilde{l}$  and  $\tilde{T}$  are in frames, such that  $l = \tilde{l}\Delta t$  results in units of seconds, where  $\Delta t$  is the frame time. Note that this is the only section of the manuscript where times are expressed in frames instead of seconds. The probability mass function of observing the entire trajectory from start to finish is  $e(\tilde{l}, \tilde{T}) = 1 - c(\tilde{l}, \tilde{T})$ . Therefore, the number of trajectories with length  $\tilde{l}$  that are experimentally observed in their entirety is  $E(\tilde{l}) = R(\tilde{l})e(\tilde{l})$ , where  $R(\tilde{l})$  is the true number of trajectories with length  $\tilde{l}$ . To account for trajectories that are truncated, the lifetime distribution is corrected,  $R(\tilde{l}) = [\tilde{T}/(\tilde{T} - \tilde{l})]E(\tilde{l})$ . The cumulative distribution function (CDF) of the CCP lifetimes is then built from  $R(\tilde{l})$  and used for model fitting.

### Model Selection for Lifetime Distribution

Bayesian information criterion (BIC) model selection was used to identify the number of subpopulations and their parameters for the CCP lifetime distributions. BIC is a popular model selection criterion, which presents a measure of fit between data and models and penalizes overparameterization (2). To avoid bias due to bin size, all models were fit to the CDF of the given data [i.e., the CDF of  $R(\tilde{l})$ ]. The BIC was minimized to select the best model:

$$\text{BIC} = n \ln(\text{RSS}/n) + p \ln(n), \quad [\text{S1}]$$

where  $n$  is the sample size, RSS is the residual sum of squares, and  $p$  is the number of free parameters (2). The model that minimizes the BIC optimizes both residuals and the number of parameters.

Exponential and Rayleigh distributions with one, two, three, and four populations were fit along with the combination of Rayleigh and exponential distributions. Equations for a single exponential, single Rayleigh, two exponential, and combination of one Rayleigh and two exponential distributions are provided below. Other combinations were built in a similar manner.

$$\text{PDF}_e(l) = \frac{1}{\tau} \exp(-l/\tau), \quad [\text{S2}]$$

$$\text{PDF}_R(l) = \frac{l}{\tau^2} \exp[-l^2/(2\tau^2)], \quad [\text{S3}]$$

$$\text{PDF}_{e+e}(l) = \frac{A}{\tau_1} \exp(-l/\tau_1) + \frac{(1-A)}{\tau_2} \exp(-l/\tau_2), \quad [\text{S4}]$$

$$\text{PDF}_{R+e+e}(l) = \frac{A_1 l}{\tau_1^2} \exp[-l^2/(2\tau_1^2)] + \frac{A_2}{\tau_2} \exp(-l/\tau_2) + \frac{(1-A_1-A_2)}{\tau_3} \exp(-l/\tau_3). \quad [\text{S5}]$$

In the equations above,  $A$  is the weight of each distribution and  $\tau_i$  is the corresponding characteristic time. For fitting purposes, the CDFs of these distributions were used. The results of the BIC model comparison are shown in Table S1.

The model that minimizes the BIC is the combination of a single Rayleigh and two exponential distributions (Eq. S5). The model consisting of two Rayleigh and one exponential distribution also yields a BIC that is close to the minimum. These two models include three subpopulations of CCP lifetimes and they agree that the shortest lifetime population is best modeled by a Rayleigh distribution, whereas the longest lifetime population is best modeled by an exponential distribution. Their discrepancy lies in the middle lifetime population. Fig. S1 displays a direct comparison between the two models. For the purpose of this manuscript, the difference between these two models is negligible. We chose to use the model with a single Rayleigh and two exponential functions, Eq. S5, due to its appearance to fit the probability density function (PDF) of CCP lifetimes better.

We find that the characteristic time constants are  $\tau_1 = 2.28 \pm 0.02$  s,  $\tau_2 = 8.6 \pm 0.2$  s, and  $\tau_3 = 45 \pm 2$  s (estimates  $\pm$  SEs). The weight of the shortest (Rayleigh) population is  $A_1 = 0.439 \pm 0.007$ , the second (exponential) population  $A_2 = 0.509 \pm 0.006$ , and the third (exponential) population  $A_3 = 1 - A_1 - A_2 = 0.052 \pm 0.004$ .

Even though a model that includes the combination of Rayleigh and exponential distributions accurately describes CCP lifetime data, there may be other empirical distributions that explain the data as well. In fact, the BIC model selection is only as good as its definition set. We have examined combinations of other distributions without finding any other successful model.

### Derivation of Trapping Model

The parameters used in this derivation are as follows:

$\alpha$	Characteristic exponent, $\alpha = K_{50}\tau_c$
$B$	Time shift in the growth of a CCP as exemplified in Fig. 1D
$k_1$	Dissociation constant between a cargo molecule and an adaptor protein
$K_f$	Fast dissociation rate from a circular domain
$K_s$	Slow dissociation rate from a circular domain
$k_{\text{off}}$	Instantaneous dissociation rate between a cargo molecule and a CCP
$l$	CCP lifetime
$N$	No. of adaptors within a CCP
$P_s$	Survival probability
$R$	Radius of a CCP
$T$	Time since initiation of the CCP
$\tau$	Binding time
$t_0$	Time at which a cargo molecule is captured
$\tau_c$	Average time interval between the arrival of two adaptor proteins to a CCP

Here, we derive a kinetic model for the interactions between CCPs and cargo. Within this model, the channel diffuses laterally across the membrane and it is randomly captured by a growing CCP by binding to an adaptor protein. It dissociates from a single adaptor according to a constant  $k_1$ . The pit cycle begins at time  $t=0$ , it grows via the addition of adaptor proteins at a rate of  $1/\tau_c$ , and it is terminated either abortively or productively at time  $t=l$  (the lifetime of the pit). After being captured in the pit, the cargo molecule remains there for a (stochastic) time  $\tau$  until it escapes. In our derivation, we first focus on the times at which the channels are captured and then on the binding times.

**(A) Times of Capture.** We obtain  $P(l|\text{capt})$ , the conditional PDF of CCP lifetimes given that cargo becomes captured within the pit, by using Bayes' theorem:

$$P(l|\text{capt}) = \frac{P(\text{capt}|l)P(l)}{P(\text{capt})}. \quad [\text{S6}]$$

$P(l)$  is experimentally measured (Fig. 1D), and to obtain  $P(\text{capt}|l)$  we integrate over the possible times of capture  $t_0$ ,  $P(\text{capt}|l) = \int_0^l P(t_0, \text{capt}|l) dt_0$ . The probability of binding at time  $t_0$  given that the pit lifetime is  $l$ ,  $P(t_0, \text{capt}|l)$ , is proportional to the perimeter of the pit. So, following our linear growth assumption,

$$P(t_0, \text{capt}|l) \sim r \sim \sqrt{N(t_0)} \sim \sqrt{(t_0+B)/\tau_c}, \quad [\text{S7}]$$

under the condition that  $0 < t_0 < l$ , where  $r$  is the radius of the pit and  $N(t)$  is the number of adaptor proteins at time  $t$ . (Eq. 1). Explicitly,

$$P(t_0, \text{capt}|l) = \begin{cases} c_1 \sqrt{t_0+B}, & 0 < t_0 < l \\ 0, & \text{otherwise} \end{cases}, \quad [\text{S8}]$$

where  $c_1$  is a normalization factor. Thus, we can find the probability of capture given the lifetime of the pit,

$$\begin{aligned} P(\text{capt}|l) &= \int_0^l P(t_0, \text{capt}|l) dt_0 = \int_0^l c_1 \sqrt{t_0+B} dt_0 \\ &= c_2 \left[ (l+B)^{3/2} - B^{3/2} \right]. \end{aligned} \quad [\text{S9}]$$

Using Eq. S6, we obtain

$$P(l|\text{capt}) = \frac{c_2}{c_B} \left[ (l+B)^{3/2} - B^{3/2} \right] P(l), \quad [\text{S10}]$$

where the a priori probability of capturing is equal to a constant,  $P(\text{capt}) = c_B$ .

Using similar arguments as those of Eq. S8, assuming that a channel binds to the pit so that  $\int_0^l P(t_0|l) dt_0 = 1$ , we find the conditional PDF of the time of capture, given a known CCP lifetime  $l$ ,

$$P(t_0|l) = \begin{cases} \frac{3}{2 \left[ (l+B)^{3/2} - B^{3/2} \right]} \sqrt{t_0+B}, & 0 < t_0 < l \\ 0, & \text{otherwise} \end{cases}, \quad [\text{S11}]$$

Then, it is straightforward to find the a priori PDF of times of capture,

$$P(t_0) = \int_{t_0}^{\infty} P(t_0|l) P(l|\text{capt}) dl = C \sqrt{t_0+B} \int_{t_0}^{\infty} P(l) dl, \quad [\text{S12}]$$

where the normalization factor is found by integration,  $C = 1/\int_0^{\infty} P(t_0) dt_0 = 3/\int_0^{\infty} 2 \left[ (l+B)^{3/2} - B^{3/2} \right] P(l) dl$ . In the main manuscript,  $P(t_0)$  is shown in Fig. 2.

**(B) Binding Times.** When a channel encounters a CCP, it is captured at the outer edge of the pit. Then, it may turn around and rapidly escape or it may explore different binding sites inside, hopping from one binding site to another. This is depicted in Fig. 4A in the main manuscript. We first derive the conditional PDF of binding times for each escape mode,  $\psi_{K_f}(\tau|t_0)$  and  $\psi_{K_s}(\tau|t_0)$ , and then we obtain the a priori PDFs of binding times,  $\psi_{K_f}(\tau)$  and  $\psi_{K_s}(\tau)$ .

*(i) Conditional probability of binding times given that the channel binds at time  $t_0$ .* We first derive the binding time for the fast-escaping population. We formulate a master equation for the survival probability, i.e., the probability the channel is still bound at time  $\tau$ ,  $dP_s/d\tau = -k_{\text{off}}P_s$ . When the escape rate is independent of pit size, this master equation yields the following:

$$P_{sK_f}(\tau|t_0, l) = \begin{cases} e^{-K_f\tau}, & 0 < \tau \leq l - t_0 \\ 0, & \text{otherwise} \end{cases}. \quad [\text{S13}]$$

The conditional PDF of stalling times is  $\psi(\tau|t_0, l) = -dP_s(\tau|t_0, l)/d\tau$ . So,

$$\psi_{K_f}(\tau|t_0, l) = \begin{cases} K_f e^{-K_f\tau} + e^{-K_f(l-t_0)} \delta(l-t_0-\tau), & 0 < \tau \leq l - t_0 \\ 0, & \text{otherwise} \end{cases}. \quad [\text{S14}]$$

Similarly, for the slowly escaping population, we formulate a master equation  $dP_s/d\tau = -K_s(\tau)P_s$ , where  $K_s$  is time dependent due to its dependence on pit size. Using the simulation results shown in Fig. 4C, we can write the slow escape rate as  $K_s(\tau) = K_{s0}/N = K_{s0}\tau_c/(\tau+t_0+B)$ . This master equation yields a power law solution  $P_{sK_s} \sim (\tau+t_0+B)^{-\alpha}$  with the associated conditional probability density for the binding times:

$$\psi_{K_s}(\tau|t_0, l) = \begin{cases} \frac{\alpha(t_0+B)^\alpha}{(\tau+t_0+B)^{1+\alpha}} + \left( \frac{t_0+B}{l+B} \right)^\alpha \delta(l-t_0-\tau), & 0 < \tau \leq l - t_0 \\ 0, & \text{otherwise,} \end{cases} \quad [\text{S15}]$$

where  $\alpha = K_{s0}\tau_c$ .

The PDF of stalling times, given the channel is captured in the pit at time  $t_0$ , is

$$\psi(\tau|t_0) = \int_{t_0}^{\infty} \psi(\tau|t_0, l) P(l|t_0) dl, \quad [\text{S16}]$$

where  $P(l|t_0) = P(l)/\int_{t_0}^{\infty} P(l') dl'$  for  $l \geq t_0$ . Then Eqs. S14 and S15 for  $K_f$  and  $K_s$ , respectively, yield the conditional PDFs of binding times for each population,

$$\psi_{K_f}(\tau|t_0) = \frac{1}{\int_{t_0}^{\infty} P(l) dl} K_f e^{-K_f\tau} \left[ \int_{t_0+\tau}^{\infty} P(l) dl + \frac{P(l=t_0+\tau)}{K_f} \right], \quad [\text{S17}]$$

and

$$\psi_{K_s}(\tau|t_0) = \frac{1}{\int_{t_0}^{\infty} P(l)dl} \left[ \frac{\alpha(t_0+B)^\alpha}{(\tau+t_0+B)^{1+\alpha}} \right] \times \left[ \int_{t_0+\tau}^{\infty} P(l)dl + \frac{(\tau+t_0+B)}{\alpha} P(l=t_0+\tau) \right]. \quad [\text{S18}]$$

(ii) The a priori probability of binding times is  $\psi(\tau) = \int_0^\infty \psi(\tau|t_0) P(t_0) dt_0$ . Using Eq. S12 together with S17 and S18 for the two populations of escape rates, we obtain the a priori PDFs of binding times,

$$\psi_{K_f}(\tau) = CK_f e^{-K_f \tau} \int_0^\infty \sqrt{t_0+B} \left[ \int_{t_0+\tau}^{\infty} P(l)dl + \frac{P(l=t_0+\tau)}{K_f} \right] dt_0, \quad [\text{S19}]$$

$$\psi_{K_s}(\tau) = C\alpha \int_0^\infty \frac{(t_0+B)^\alpha \sqrt{t_0+B}}{(\tau+t_0+B)^{1+\alpha}} \times \left[ \int_{t_0+\tau}^{\infty} P(l)dl + \frac{(\tau+t_0+B)}{\alpha} P(l=t_0+\tau) \right] dt_0, \quad [\text{S20}]$$

where  $C$  is defined in Eq. S12.

At last, we combine the two distributions, Eqs. S19 and S20, with a weight  $w$ , such that  $\psi(\tau) = w\psi_{K_f}(\tau) + (1-w)\psi_{K_s}(\tau)$ . As determined from our escape-time Monte Carlo simulations, the weight of the fast-escaping population is  $w = 0.75$ . Then,

$$\psi(\tau) = wCK_f e^{-K_f \tau} \int_0^\infty \sqrt{t_0+B} \left[ \int_{t_0+\tau}^{\infty} P_{\text{fast}}(l)dl + \frac{P(l=t_0+\tau)}{K_f} \right] dt_0 + (1-w)C\alpha \int_0^\infty \frac{(t_0+B)^\alpha \sqrt{t_0+B}}{(\tau+t_0+B)^{1+\alpha}} \times \left[ \int_{t_0+\tau}^{\infty} P_{\text{slow}}(l)dl + \frac{(\tau+t_0+B)}{\alpha} P(l=t_0+\tau) \right] dt_0, \quad [\text{S21}]$$

where  $P_{\text{fast}}(l) = A_1 P_1(l) + A_2 P_2(l) + A_3 P_3(l)$  is the CCP lifetime distribution used for the fast-escaping channels and, similarly,  $P_{\text{slow}}(l) = A_1^* P_1(l) + A_2^* P_2(l) + A_3^* P_3(l)$  for the slow-escaping population.  $P_1(l)$  corresponds to the short-lived CCP lifetimes, found to be Rayleigh distributed;  $P_2(l)$  is the second population of exponentially distributed lifetimes; and  $P_3(l)$  is the long-lived exponentially distributed population.  $A_1, A_2,$  and  $A_3$  are the weights of the CCP lifetime populations, as found above in *Model Selection for Lifetime Distribution*. Naively,  $(A_1^*, A_2^*, A_3^*) = (A_1, A_2, A_3)$ , as shown by the green line in Fig. S2. However, in the last stages of a productive CCP, the interior of the pit may not accept any more cargo molecules. When the whole distribution of CCPs is used, we observe that the expected binding times are much longer than what the data show (Fig. S2). To adjust for this effect, the long-lived population of CCPs was removed from the contribution to the power law distribution in Eq. S21. This is simply achieved by setting  $A_3^* = 0$  (red line in Fig. S2). Alternatively, one may consider the possibility that the later CCP stages contribute (minimally) to the power law distribution. Thus, we can adjust  $A_3^*$  to include this small contribution. We find that the value that best describes the experimental data is  $A_3^* = 5 \times 10^{-5}$ . The blue curve in Fig. S2 provides the result with this final adjustment, i.e., allowing the long-lived CCPs to contribute only 0.005% to the power law behavior of binding times.

1. Loerke D, et al. (2009) Cargo and dynamin regulate clathrin-coated pit maturation. *PLoS Biol* 7(3):e57.

2. Barkard RE, Çela E (1999) *Handbook of Combinatorial Optimization*, eds Du DZ, Pardalos PM (Kluwer Academic Publishers, Dordrecht, The Netherlands), pp 75–149.

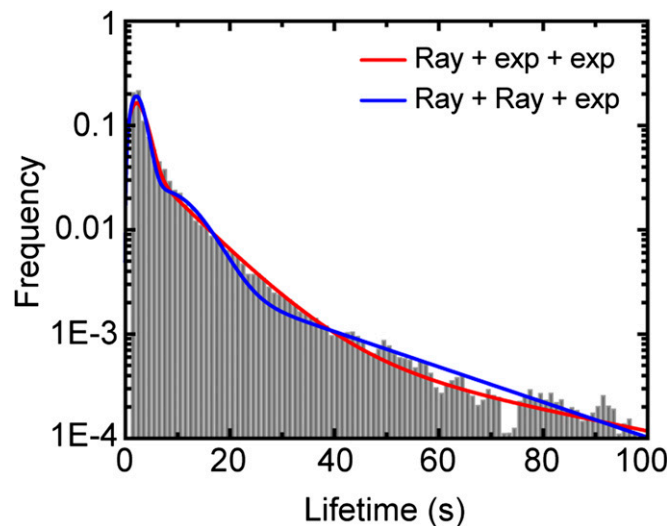
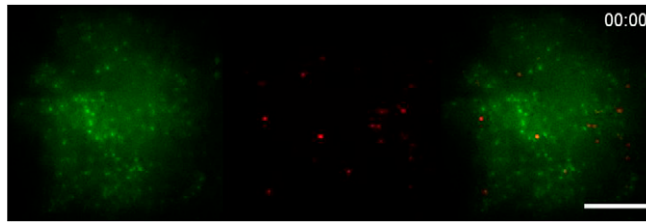


Fig. S1. Comparison of CCP lifetime models. Shown in blue is a combination of two Rayleigh and one exponential distribution, and in red, a combination of one Rayleigh and two exponential distributions, as in Eq. S5. In both cases, the shortest population is modeled by a Rayleigh distribution and the longest population by an exponential distribution.

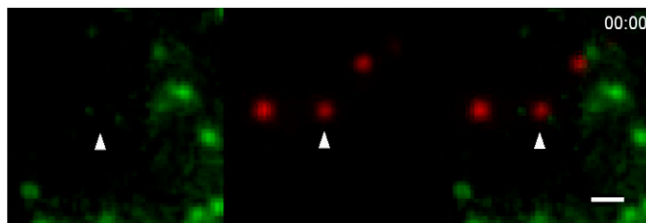




**Movie S1.** Quantum dot (QD)-Kv2.1 and GFP-clathrin light chain (CLC) fluorescence. Fluorescently labeled Kv2.1 and clathrin on the basal surface of a HEK293 cell. The left panel is GFP-CLC fluorescence (green) only, the middle panel is the fluorescence of QD-labeled Kv2.1 (red), and the right panel is the overlay of the two images. Kv2.1 channels inherently display two types of motion on the cell surface: a majority of Kv2.1 channels are retained within membrane compartments, whereas a fraction freely diffuses across the surface (see ref. 1). Consequently, some QD-labeled channels appear to be quite mobile, whereas others are confined to smaller areas. GFP-labeled endocytic pits appear as distinct, diffraction-limited fluorescent puncta. The more mobile Kv2.1 channels are seen to alternate between diffusing and stalling modes. The stalls occur on top of clathrin spots. (Scale bar: 10  $\mu\text{m}$ .)

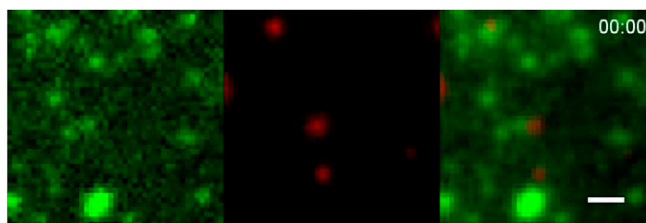
1. Weigel AV, Simon B, Tamkun MM, Krapf D (2011) Ergodic and nonergodic processes coexist in the plasma membrane as observed by single-molecule tracking. *Proc Natl Acad Sci USA* 108(16):6438–6443.

#### [Movie S1](#)



**Movie S2.** Cargo capture and endocytosis. The left panel is GFP-CLC fluorescence, the middle panel is QD-Kv2.1 fluorescence, and the right panel is their overlay. The movie depicts the capture of a Kv2.1 cargo molecule into a newly forming endocytic pit. The cargo remains captured within the pit until it is internalized. The white arrow marks the location of the newly forming pit. The QD-Kv2.1 channel becomes captured into the pit shortly during the initial stages of the CCP and remains there until it is endocytosed at 28 s. Both the QD-labeled channel and GFP-labeled CCP flicker before complete internalization due to their random motion into and out of the TIRF illumination field. Also seen in the movie is a freely diffusing QD-Kv2.1 channel. This channel becomes transiently captured into the pit at 18 s. However, it escapes before the CCP is internalized. (Scale bar: 1  $\mu\text{m}$ .)

#### [Movie S2](#)



**Movie S3.** Capture and release of cargo into endocytic pits. Similar to [Movies S1](#) and [S2](#), GFP-CLC fluorescence is shown in the left panel, QD-Kv2.1 fluorescence, in the middle panel, and their overlay, in the right panel. The movie displays the capturing of cargo (Kv2.1) into endocytic pits. Capturing events lasting longer than 0.5 s are marked with yellow arrows. Also, here, both freely diffusing and confined Kv2.1 channels are seen. (Scale bar: 1  $\mu\text{m}$ .)

#### [Movie S3](#)